REPORT DOCUMENTATION PAGE

Form Approved
OMB No. 0704-0188

1. REPORT DATE *(DD-MM-YYYY)*	2. REPORT TYPE	3. DATES COVERED *(From - To)*
22-08-2014	Final Report	11/12/2009-02/28/2014

4. TITLE AND SUBTITLE
The Electromagnetic and Mechanical Properties of Structural Composites: A Theoretical and Experimental Design Study

5a. CONTRACT NUMBER
N00014-10-1-0325

5b. GRANT NUMBER

5c. PROGRAM ELEMENT NUMBER

6. AUTHOR(S)
Mark Mirotznik and Shridhar Yarlagadda

5d. PROJECT NUMBER

5e. TASK NUMBER

5f. WORK UNIT NUMBER

7. PERFORMING ORGANIZATION NAME(S) AND ADDRESS(ES)
University of Delaware
210 Hullihen Hall
Newark, DE 19716

8. PERFORMING ORGANIZATION REPORT NUMBER
CYBR33211210000

9. SPONSORING / MONITORING AGENCY NAME(S) AND ADDRESS(ES)
Office of Naval Research
Linda Shipp
703-696-8559
linda.shipp@navy.mil

10. SPONSOR/MONITOR'S ACRONYM(S)
ONR

11. SPONSOR/MONITOR'S REPORT NUMBER(S)

12. DISTRIBUTION / AVAILABILITY STATEMENT
Approved for Public Release, distribution unlimited

13. SUPPLEMENTARY NOTES

14. ABSTRACT

In this ONR funded project investigators at the University of Delaware's Department of Electrical and Computer Engineering and Center for Composite Materials developed and validated new models to predict the electromagnetic properties of woven fabric composites over a broad frequency range.

15. SUBJECT TERMS

16. SECURITY CLASSIFICATION OF:			17. LIMITATION OF ABSTRACT	18. NUMBER OF PAGES	19a. NAME OF RESPONSIBLE PERSON
a. REPORT	b. ABSTRACT	c. THIS PAGE			Mark Mirotznik
U	U	U	UU	24	19b. TELEPHONE NUMBER *(include area code)* 302-831-4241

Final Technical Report
N00014-11-1-0325

Name of Institute: The University of Delaware

Title of Project: "The Electromagnetic and Mechanical Properties of Structural Composites: A Theoretical and Experimental Design Study"

PI Information:
Mark S. Mirotznik, Associate Professor
Department of Electrical and Computer Engineering
The University of Delaware
106 Evans
Newark, Delaware 19716

Tel: (302) 831-4241
Fax: (302) 831-4316
Cell: (301) 873-7029
mirotzni@ece.udel.edu

Co-PI Information:
Shridhar Yarlagadda, Assistant Director of Research
Center for Composite Materials
The University of Delaware
Newark, DE 19716

Tel: (302) 831-4941
Fax: (302) 831-8525

yarlagad@udel.edu

ONR POC:
Dr. Steven J. Russell
Office of Naval Research, Code 331
Ships & Engineering Systems Division
875 North Randolph Street
Arlington, VA 22203-1995
Phone: (703) 696-4714 | Fax: (703) 696-0934 | Cell: (703) 785-8028
steven.j.russell@navy.mil

THE ELECTROMAGNETIC AND MECHANICAL PROPERTIES OF STRUCTURAL COMPOSITES: A THEORETICAL AND EXPERIMENTAL DESIGN STUDY

FINAL TECHNICAL REPORT

1.0 Abstract

In this ONR funded project investigators at the University of Delaware's Department of Electrical and Computer Engineering and Center for Composite Materials developed and validated new models to predict the electromagnetic properties of woven fabric composites over a broad frequency range.

2.0 Introduction and Background

The U.S. Navy is moving towards a vision of integrated ship topside where antennas will be an integral part of the load carrying structure. This integrated multi-functional structure combines both structural and electromagnetic requirements, while meeting other topside integration requirements including signature control and isolation.

To accomplish this goal will require the marriage of traditional ship materials, such as structural composites, with radiating antenna elements, frequency selective surfaces and other electromagnetic based components. In doing so it will be necessary that these materials maintain their mechanical properties while creating an electromagnetic environment (e.g. low loss, wideband, isotropic ...) that is conducive for efficient radiating systems and other electromagnetically based applications.

During a previous ONR funded effort the PI has shown that it is feasible to create composite materials with "engineered" electromagnetic properties by pattering their surface on a subwavelength scale. Using this approach a number of composite samples were designed and experimentally validated to have nearly zero reflected losses over a wide band of frequencies and incident angles. However, while reflective losses were minimized using this approach, material losses were still present and in some cases would pose significant difficulties in integrating antenna elements either within or behind structural composites. In this project investigators from the University of Delaware's Department of Electrical and Computer Engineering (ECE) and the Center for Composite Materials (UD-CCM), in collaboration with the Naval Surface Warfare Center, Carderock Division, conducted a comprehensive theoretical and experimental study on the electromagnetic and mechanical properties of structural composites. This resulted in a new and validated numerical model for predicting the electromagnetic properties of woven fabric composites over a very large frequency band. We were able to use this model and the experimental measurements to create a "recipe book" or set of design tools that can be used by Navy scientists and

engineers to optimize the electromagnetic and mechanical properties of composites for any particular application.

3.0 New Electromagnetic Model of Woven Fabric Composites

Woven fabric composites are a popular core building block material of many commercial and military platforms in addition to being a common substrate for circuit board manufacturing. The composite's high strength to weight ratio, low cost and good thermal properties are among some reasons for their popularity. Conventional composites are composed of layers of woven fabrics, usually consisting of glass, polymer or carbon fibers that are held together by a polymer matrix or resin. Decades of military, academic and industrial research have gone into the design and manufacturing of composites whose mechanical properties are optimized. Much more recently, material researchers have begun to investigate ways to create composites that have other attractive material properties beyond their mechanical strength, such as electromagnetic (EM) properties. By tailoring the electromagnetic properties of structural composites (e.g. complex permittivity and permeability), it may be possible to integrate antennas, frequency selective surfaces and other electromagnetic components directly into the structural skin of future commercial and military vehicles and structures. Such applications would be greatly aided by good predictive models that could be used to select the proper base materials (i.e. fabric type, fabric architecture and resin) and layered configuration to create a structural composite with attractive electromagnetic and mechanical properties. The literature reports several approaches for simulating the electromagnetic properties of woven composites. The first uses effective media theory to provide closed form approximations for the composite's effective dielectric constant as a function of the dielectric properties of the fiber and resin components and the geometrical architecture of the fabric. Although attractive from a computational perspective, effective media theory is accurate only for fabric architectures in which the length scales (i.e. fabric's unit cell size) are much smaller than the wavelength of illumination. As the wavelength approaches the periodicity of the fabric, referred to as the resonance regime, the assumptions on which these closed form expressions are based are no longer valid. For most structural fabrics, this occurs well within the microwave region, and for composite substrates used in circuit boards, the resonance regime shifts to even higher frequencies due to weaves with smaller unit cells.

A second predicts the dielectric properties of unidirectional composite fabrics and laminates by constructing equivalent lump circuit representations. The circuit models, consisting of parallel RC circuits, were shown to accurately predict the effective dielectric properties of composite laminates within the X-band (8-12 GHz). The circuit analog method becomes less accurate as the frequency increases to the point in which the wavelength approaches the unit cell size.

A third approach utilizes rigorous electromagnetic models. Although computationally more difficult, this approach can generate accurate results for woven composites of any fabric architecture. Several different rigorous electromagnetic methods can be used for this purpose, including the finite element method (FEM), finite difference time domain (FDTD) and modal based solution methods, such as the rigorous coupled wave (RCW) algorithm. The major disadvantage of employing rigorous methods is the computational expense. A FEM model that incorporates the exact geometry of the unit cell, including the fiber bundle, requires hours of computation time on a medium sized workstation.

In our model we developed a hybrid electromagnetic model that combines effective media theory with a

rigorous electromagnetic method (i.e. RCW method). The end result is a computationally efficient model that predicts the electromagnetic properties of woven fabric composites, including resonance effects, at frequencies as high as 50 GHz. Moreover, this method can be easily applied to complicated 2D and 3D weave architectures and to multilayered laminates. In this project, experimental validation from 4-50 GHz is provided for single layers of dry structural grade woven glass fabrics and for the same fabrics infused with a vinyl ester resin.

WOVEN FABRIC ARCHITECTURES

Fiber-reinforced plastic (FRP) structures use a large variety of structural grade woven fabrics. These fabrics vary in fiber type (e.g. glass, carbon, kevlar or aramid), thickness, weight and geometrical architecture of the weave. For most applications, a number of fabric layers are stacked in specific orientations and infused with a polymer resin (e.g. thermosets such as epoxy, vinyl ester or polyester) to create a FRP structure that satisfies the mechanical requirements of the application. In creating electromagnetically functionalized composite structures, choice of the proper fabrics and resins must also take into account the electromagnetic requirements (e.g. low loss, low scattering, etc.). The broadband electromagnetic properties are sensitive to the choice in fiber type, weave, bundle size and bulk dielectric properties of the resin.

The most common weave architectures are shown in Figure 1. These include unidirectional and common two-dimensional weaves. A unidirectional fabric, shown in Figure 1a, is composed of a periodic arrangement of fiber bundles aligned along the same axis. It should be noted that each fiber bundle, shown in the figure, is actually composed of thousands of small cylindrical fibers. The cross sectional shapes of the bundles typically form elongated ellipses with an eccentricity close to unity.

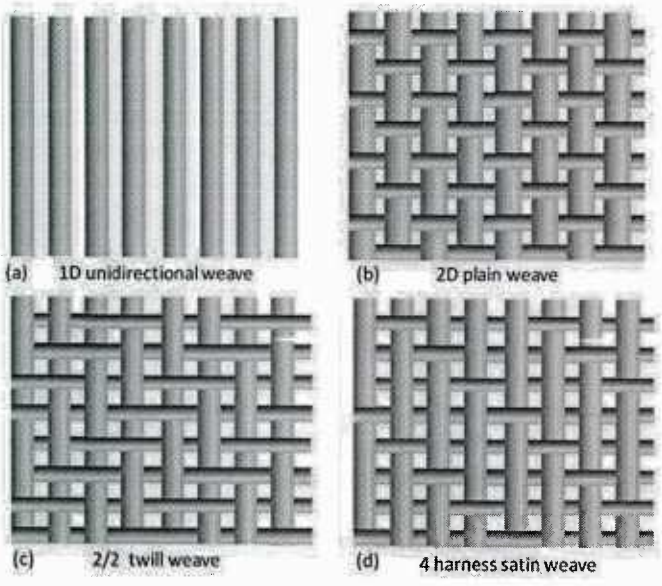

Figure 1. Common weave architectures used in woven fabric structural composites.

In two-dimensional weaves, the fiber bundles are aligned along two orthogonal axes. The most common two-dimensional weaves are the plain, twill and satin weaves (Figure 1b through 1d, respectively). There are a number of other 2D and 3D weave types that can also be modeled using the methods described previously. Here we concentrate on modeling only single layer fabrics - both dry and infused with a polymer resin. However, the described methods can easily be applied directly to the analysis of multi-layered composite laminates.

APPROXIMATE ELECTROMAGNETIC REPRESENTATION

In this section, we describe the approximate electromagnetic representations of the woven fabric composites. The objectives of the model are: (1) to create an EM model that accurately predicts the

electromagnetic response of a woven fabric composite over a broad range of frequencies (DC-50 GHz) where effective media theory becomes invalid, (2) to create an EM model that can be applied directly to a wide variety of fabric and resin types and weave architectures, and (3) to create a model that is computationally efficient and can be integrated subsequently into an iterative design algorithm.

Our approach was to combine effective media theory, where valid, with an efficient rigorous EM algorithm. To this end, we employed the following approximations to model a single woven fabric layer. We assumed that:

(1) The fabric weave has adequate uniformity so that it can be modeled as an infinitely periodic structure.
(2) The dielectric properties of the individual fiber bundles shown in Figure 1a-1d can be approximated by their effective bulk anisotropic properties. This is a reasonable approximation for the frequencies of interest here (i.e. <50 GHz) since the diameter and spacing of the individual fibers is very small compared to the wavelength. The specific effective media model used for the fiber bundles is discussed in more detail later.
(3) For regions in which two fiber bundles overlap, such as the 2D weaves shown in Figure 1b-1d, the electromagnetic properties are insensitive to the order (i.e. insensitive to which bundle is on the top) . Moreover, the dielectric properties within the overlap region are assumed to be an average of the x-directed and y-directed fiber bundle properties. This is a reasonable approximation as long as the thickness of the fiber bundle is small compared to the wavelength. For most structural grade fabrics, the bundle thickness is less than <0.5 mm. Consequently, this approximation will begin to break down as the frequency increases much beyond 50 GHz.
(4) The cross sectional shape of the fiber bundle, which is typically an elongated ellipse, can be approximated as a rectangular cross-section of the same cross-sectional area. This is again a reasonable assumption as long as the thickness of the fiber bundle is thin compared to the wavelength.

With these approximations in mind, the electromagnetic representations for the unidirectional and 2D weaves shown in Figure 1 are now presented.

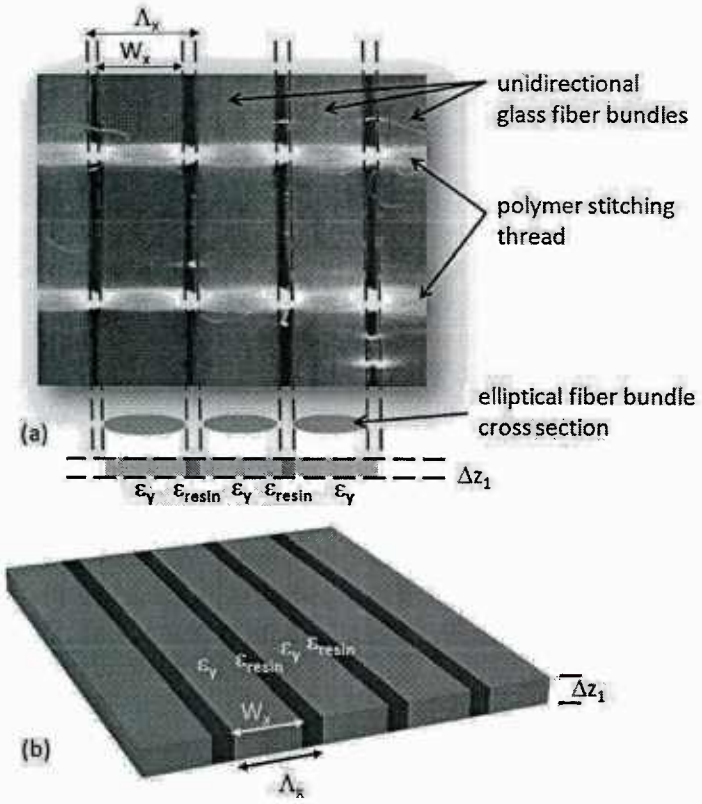

Figure 2. Electromagnetic model used to analyze unidirectional composite fabrics.

Unidirectional fabrics

Figure 2a shows a typical unidirectional composite fabric. It also shows the thin polymer stitching thread used to hold the fiber bundles in place. The stitching thread takes up less than 2% of the total fabric volume and, as a result, its contribution to the fabric's electromagnetic properties was considered negligible. Figure 2a illustrates a single layer of a dry fabric in which all spaces not occupied by a fiber, both internal to a fiber bundle and between fiber bundles, are assumed to be free-space. However, in the vast majority of applications, this fabric is infused with a resin that fills in all these unoccupied spaces.

Figure 2b shows the approximate electromagnetic representation of the unidirectional fabric. Here we applied three of the approximations listed previously. Namely, that the electromagnetic properties of the fiber bundles were modeled as an effective anisotropic material and that the cross sectional geometry of the fiber bundles was approximated using a rectangular geometry. It is clear that for the unidirectional fibers our electromagnetic representation is simply a 1D dielectric grating with anisotropic material properties.

Two dimensional woven fabrics – four region model

Figure 3 illustrates a standard orthogonal 2D woven composite fabric with a plain weave. It is constructed with two sets of orthogonal fiber bundles running along the x and y axis. The approximate electromagnetic representation of this fabric is presented in Figures 3 and 4. Applying the four approximations described previously, we construct a unit cell composed of four regions. Region 1 is the portion of the fabric in which the x-directed and y-directed fiber bundles overlap; regions 2 and 3 contain only the y-directed and x-directed fiber bundles, respectively; and region 4 is completely unoccupied by fibers. To account for the region where the fiber bundles overlap, the total thickness of the unit cell is twice the thickness of the fiber bundle (i.e. 2 s periodically replicated with periods of Λ_x and Λ_y along the x and y axes, respectively.

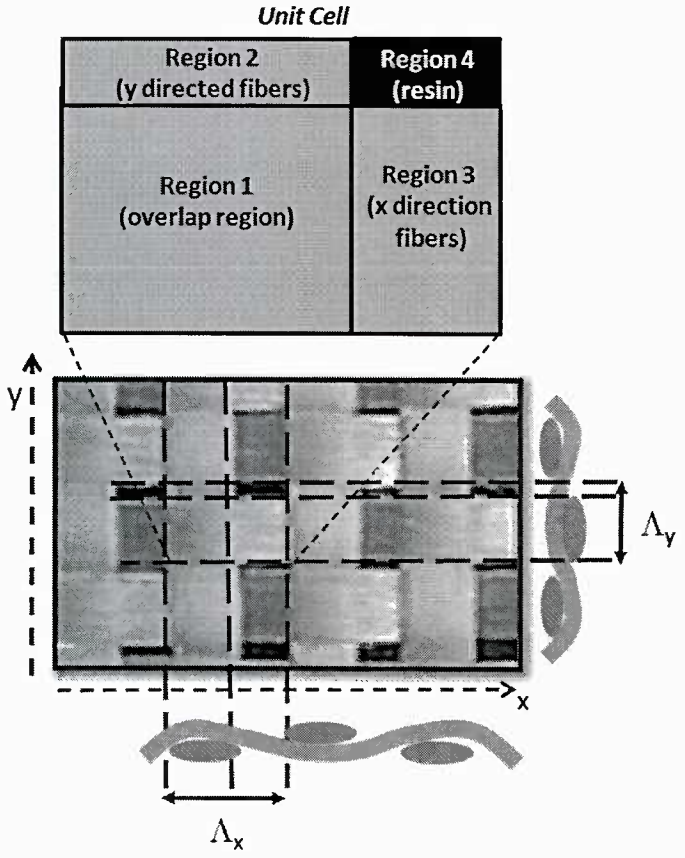

Figure 3. Planar view of the 4-region model used to represent the unit cell of 2D woven fabrics. The fabric is assumed to be infinitely periodic in both the x and y directions with a periodicity of $_x$ and $_y$, respectively. In should be noted that the periods along the x and y axes may not be identical as weaves can be non-symmetric. This could lead to anisotropic electromagnetic properties.

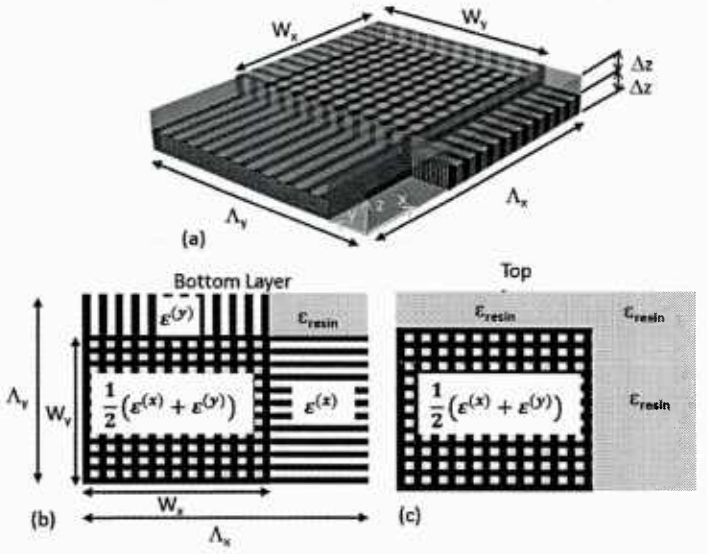

Figure 4. (a) Detailed 3D view of the 4-region model used to model the fabric's unit cell. In the z-direction the model is composed of two equally thick layers with dielectric properties shown in (b) and (c).

In the z-direction, each unit cell is broken into two equally thick layers (Figure 4a). The thickness of each layer is assumed to be the thickness (z) of a fiber bundle. The bottom layer (Figure 4b) contains the non-overlapping fiber bundles as well as the overlapping region. The top layer (Figure 4c) only contains the overlapping region. All regions unoccupied by fibers are assumed to be filled with air (fabric model) or resin (composite model). Figure 4 shows the dielectric properties within each of the various regions. Specifically, $\bar{\bar{\varepsilon}}_1$, $\bar{\bar{\varepsilon}}_2$, $\bar{\bar{\varepsilon}}_3$ and ε_4 denotes the effective permittivity in each of the four regions illustrated in Figures 3 and 4. In regions 2 and 3 the permittivity will depend on the orientation of the fiber bundle (e.g. x or y directed fibers) and the polarization of the incident field (e.g. x or y linear polarization). This can be described mathematically as permittivity tensors given by

(1)

$$\bar{\bar{\varepsilon}}_2 = \begin{bmatrix} \varepsilon_x^{(y)} & 0 \\ 0 & \varepsilon_y^{(y)} \end{bmatrix}$$
$$\bar{\bar{\varepsilon}}_3 = \begin{bmatrix} \varepsilon_x^{(x)} & 0 \\ 0 & \varepsilon_y^{(x)} \end{bmatrix}$$

where the superscripts in (1) refer to the orientation of the fibers and the subscripts denotes the polarization state of the incident field. For the case in which the fiber bundles oriented in the x and y directions are identical (the most common case) then $\varepsilon_x^{(x)} = \varepsilon_y^{(y)}$ and $\varepsilon_x^{(y)} = \varepsilon_y^{(x)}$. In region 1 of Figure 3 (i.e. overlapping region) we assume the effective permittivity is simply an average of regions 2 and 3 and is given by

$$\bar{\bar{\varepsilon}}_1 = \frac{1}{2}(\bar{\bar{\varepsilon}}_2 + \bar{\bar{\varepsilon}}_3)$$

(2)

In region 4 the permittivity is scalar equal to the bulk properties of the resin, $_4 = _{resin}$. The proposed unit cell description is similar to "mosaic model" used in fabric mechanical property prediction models . In the

end, the 4-region model of 2D woven fabrics resembles a double periodic dielectric grating structure in which the dielectric properties within the grating are the effective anisotropic properties described above. Once the effective properties are calculated, the electromagnetic response of the grating can be determined using a rigorous electromagnetic algorithm described in more detail later.

It should be noted that the electromagnetic representation for 2D woven fabrics remains the same across the standard weave configurations shown in Figure 1. This results from the fact that the only variation between these weaves is the order, in which the fiber bundles overlap. Since we are assuming that the EM properties are insensitive to that order the same general model can be employed. Experimental validation for this assumption is provided later in this report.

Effective Dielectric Constant of Individual Fiber Bundles

Each fiber bundle within a composite fabric is itself a heterogeneous mixture of thousands of individual cylindrical fibers packed within a background material or resin (Figure 5). If we assume that the diameter of each individual fiber is small compared to the wavelength, then we can employ effective media theory to represent the bundle properties as an effective anisotropic bulk medium. Since the diameter of most standard glass or carbon fibers within structural composites is less than 25 μm, this is a reasonable assumption well into the millimeter or even terahertz frequency regimes.

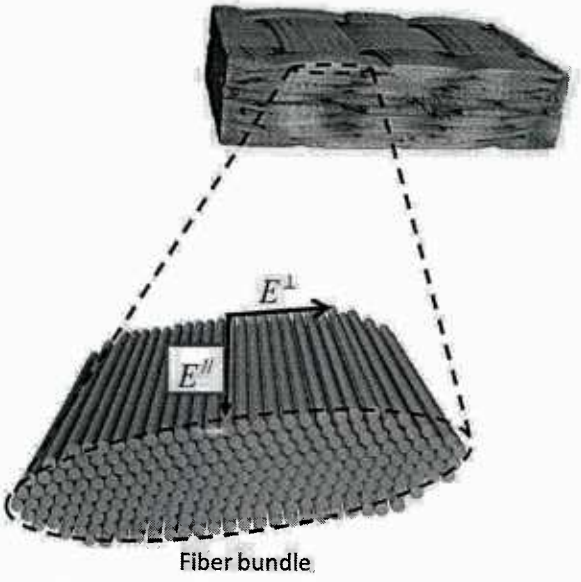

Figure 5. Illustration of fiber bundles used to create the woven fabrics. Each bundle is comprised of thousands of individual cylindrical fibers.

A number of investigators have explored effective media approximations of composite systems that we can apply to our system. Of those formulas, Bruggeman's approximation for 2D parallel cylinders was the most representative of the fiber bundles encountered in structural composite fabrics. Without any loss in generality we will assume the fiber bundles to be oriented along the x-axis. Bruggeman's formula calculates the effective anisotropic dielectric properties when the electric field is polarized parallel to the fiber direction as

$$1 - v_f = \frac{\varepsilon_{fiber} - \varepsilon_x^{(x)}}{\varepsilon_{fiber} - \varepsilon_{resin}} \left(\frac{\varepsilon_{resin}}{\varepsilon_x^{(x)}} \right)^{1/2} \tag{3}$$

where v_f denotes the volume fraction of fiber within the bundle, ε_{fiber} and ε_{resin} denote the bulk permittivity of the fiber and resin components, respectively, and $\varepsilon_x^{(x)}$ represents the effective permittivity for the case of an x-directed fiber bundle with the incident field polarized parallel to the axis of the fibers. If the incident electric field vector is oriented perpendicular to the fiber axis, then the effective media approximation is simply given as a straight volume fraction average.

$$\varepsilon_y^{(x)} = v_f \cdot \varepsilon_{fiber} + (1 - v_f)\varepsilon_{resin} \tag{4}$$

where $\varepsilon_y^{(x)}$ represents the effective permittivity of the x-directed fiber bundle for the perpendicular polarization case.

The properties for the y-directed fiber bundles of (1) are easily derived from (3) and (4) by a simple substitution of "x for y" and "y for x". It should be noted that the effective dielectric properties of the fiber bundles, calculated using (1) through (4), are reasonably sensitive to the bundle's volume fraction of fiber to resin, v_f. Unfortunately, there is always some uncertainty in determining $_f$. In theory, the maximum theoretical value of v_f for a tightly hexagonally packed bundle is 92%. However, in reality the bundles are never perfectly formed and the volume fraction can be as low at 60%. To arrive at a more accurate estimate, we used cross-sectional microscopy to measure v_f for a number of fiber bundles. The micrograph image of Figure 6 illustrates the imperfect arrangement of fibers within a typical bundle. Based on a statistical sampling of various fiber bundle measurements, we arrived at an average volume fraction of fiber-to-resin of 70%. Thus, throughout the remainder of this report, we assume $v_f = 0.7$ for all numerical simulations.

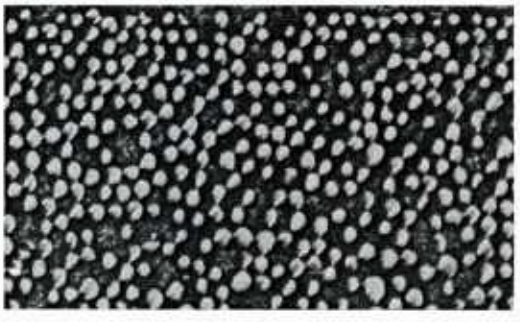

Figure 6. Micrograph image of the cross section of a typical fiber bundle. The white objects denote the fibers. The image clearly indicates that fiber packing is far from ideal.

It should be noted that Bruggeman's formula is applied only for the case of non-twisted fiber bundles. While we believe the model will still be accurate in the case of fabrics in which the fiber bundles have a slight twist, it would likely need to be revised for the case of highly twisted bundles (e.g. rope like bundles). Fortunately, the vast majority of structural fabrics do not have twisted bundles.

ELECTROMAGNETIC MODELING OF WOVEN FABRIC

A. Rigorous Coupled Wave Analysis

To predict the wideband electromagnetic properties of woven fabric composites using the models shown in Figures 2 and 4, we chose to implement the rigorous coupled wave (RCW) algorithm originally presented by Moharam and Gaylord.

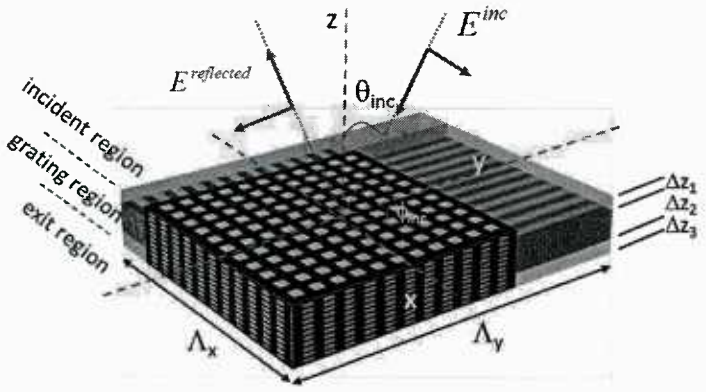

Figure 7. Solution domain used by the rigorous coupled wave theory to solve for the reflected and transmitted fields from woven fabric composites.

Using this method, we define regions within the solution domain illustrated in Figure 7. These are (1) *an incident region* that is assumed to be an infinite half-space filled with a lossless dielectric of index n_{inc}, (2) *an exit region* that is assumed to be another infinite half-space filled with a lossless dielectric of index n_{exit}, and (3) *a layered grating region* that contains multiple layers of dielectric slabs with periodic structures. The total thickness of the layered region is

$$Z_{tot} = \sum_{n=1}^{N} \Delta z_n \qquad (5)$$

where Δz_n denotes the thickness of each layer and N denotes the total number of layers. The first step in the RCW method is to represent the electromagnetic fields in each of the three regions.

Incident Region

Within the incident region, denoted as region I, the electromagnetic fields consist of an incident plane wave plus all of the diffracted orders reflected from the structure. This is written for the electric fields as

$$\vec{E}_I = \hat{u}\ \exp(-j\vec{k}_I \cdot \vec{r}) + \sum_{m=-\infty}^{\infty} \sum_{n=-\infty}^{\infty} \vec{R}_{mn} \exp(-j(\vec{k}_{I,mn} \cdot \vec{r})) \quad (6)$$

where $\vec{k}_I$ and $\hat{u}$ denote the wave vector and unit polarization vector of the incident plane wave, respectively. The second term in (6) accounts for all the reflected diffractive orders. Since each of the components in (6) represents a plane wave, the magnetic field equations can be easily derived from these. In Equation (6), $\vec{R}_{mn}$ and $\vec{k}_{I,mn}$ denote the vector reflection coefficient and wave vector of the mn-th reflected order in region I, respectively. The vector components of $\vec{k}_{I,mn}$, result from the phase matching and Floquet conditions, and are given by

$$\vec{k}_{I,mn} = \hat{u}_x \left[k_o n_{inc} \sin(\theta_{inc}) \cos(\phi_{inc}) - \frac{2\pi m}{\Lambda_x} \right] + \hat{u}_y \left[k_o n_{inc} \sin(\theta_{inc}) \sin(\phi_{inc}) - \frac{2\pi m}{\Lambda_y} \right] - \hat{u}_z k_{Iz,mn} \quad (7)$$

where θ_{inc} is the polar angle and ϕ_{inc} is the azimuth angle of the incident plane wave.

The z component of the wave vector, given in (7), is written more explicitly as

$$k_{zI,mn} = \begin{cases} \sqrt{(n_{inc}k_o)^2 - k_{x,m}{}^2 - k_{y,n}{}^2}, & k_{x,m}{}^2 + k_{y,n}{}^2 < (n_{inc}k_o)^2 \\ -j\sqrt{k_{x,m}{}^2 + k_{y,n}{}^2 - (n_{inc}k_o)^2}, & k_{x,m}{}^2 + k_{y,n}{}^2 > (n_{inc}k_o)^2 \end{cases} \quad (8)$$

where $k_{x,m}$ and $k_{y,n}$ denote the x and y component of the wave vector given in (7). It is easily deduced from (7) and (8) that, if the grating periods Λ_x and Λ_ψ are small compared to the incident wavelength (λ /n_{inc}), only the (m=n=0) diffractive order will propagate in reflection and transmission (i.e. all other diffractive orders will be evanescent). This condition is written mathematically as

$$\Lambda_x < \frac{\lambda_o}{n_{inc}(1-\sin(\theta_{inc})\cos(\phi_{inc}))}, \; \Lambda_y < \frac{\lambda_o}{n_{inc}(1-\sin(\theta_{inc})\sin(\phi_{inc}))} \quad (9)$$

Exit Region

Within the exit region, denoted as region III, the electromagnetic fields consist of all the diffracted orders transmitted through the structure. This is written for the electric fields as

$$\vec{E}_{III} = \sum_{m=-\infty}^{\infty}\sum_{n=-\infty}^{\infty}\vec{T}_{mn}\exp(-j(\vec{k}_{III,mn}\cdot\vec{r})) \quad (10)$$

Here $\vec{T}_{mn}$ and $\vec{k}_{III,mn}$ denote the vector transmission coefficient and wave vector of the mn-th transmitted order in region III, respectively. The wave vector in region III takes the same mathematical form as (7) and (8) with the one exception of replacing n_{inc} with n_{exit}. Using a similar analysis to that of region I, it can easily be shown that, to avoid any propagating diffractive orders in the transmitted region other than the m=n=0 term, the grating periods must satisfy the relations

$$\Lambda_x < \frac{\lambda_o}{n_{exit}(1-\sin(\theta_{inc})\cos(\phi_{inc}))}, \; \Lambda_y < \frac{\lambda_o}{n_{exit}(1-\sin(\theta_{inc})\sin(\phi_{inc}))} \quad (11)$$

Multi-layered grating region

Between the incident and exit regions is a unit cell of the woven fabric composite models illustrated in Figures 2 and 4.

In the RCW method, the electric and magnetic fields within each layer of the grating region, denoted by the superscript p, are written as a Fourier expansion of spatial harmonics given by

$$\begin{aligned} \vec{E}_{II}^{\,p} &= \sum_{m=-\infty}^{\infty}\sum_{n=-\infty}^{\infty}\vec{S}_{mn}^{\,p}(z)\exp(-j(k_{xm}x + k_{yn}y)) \\ \vec{H}_{II}^{\,p} &= -j\sqrt{\frac{\varepsilon_o}{\mu_o}}\sum_{m=-\infty}^{\infty}\sum_{n=-\infty}^{\infty}\vec{U}_{mn}^{\,p}(z)\exp(-j(k_{xm}x + k_{yn}y)) \end{aligned} \quad (12)$$

where $\vec{U}_{mn}^{\,p}(z)$ and $\vec{S}_{mn}^{\,p}(z)$ represent the amplitudes of the spatial harmonics in the p^{th} layer for the magnetic and electric fields respectively [16]. Substituting (12) into Maxwell's two curl equations and eliminating the z component results in the following coupled system of first order differential equations for the spatial harmonic amplitudes of (12).

$$\frac{\partial S^p_{ymn}(z)}{\partial z} = U^p_{xmn}(z) + \frac{k_{ym}}{k_o^2}\sum_{q=-\infty}^{\infty}\sum_{r=-\infty}^{\infty}\xi^p_{m-r,n-q}(-k_{yq}U^p_{xrq} + k_{xr}U^p_{yrq})$$

$$\frac{\partial S^p_{xmn}(z)}{\partial z} = -U^p_{ymn}(z) + \frac{k_{xm}}{k_o^2}\sum_{q=-\infty}^{\infty}\sum_{r=-\infty}^{\infty}\xi^p_{m-r,n-q}(-k_{yq}U^p_{xrq} + k_{xr}U^p_{yrq}) \quad (13)$$

$$\frac{\partial U^p_{ymn}(z)}{\partial z} = \sum_{q=-\infty}^{\infty}\sum_{r=-\infty}^{\infty}\varepsilon^p_{m-r,n-q}S^p_{xrq} + \frac{k_{ym}}{k_o^2}\left(k_{xm}S^p_{ymn} - k_{yn}S^p_{xmn}\right)$$

$$\frac{\partial U^p_{xmn}(z)}{\partial z} = -\sum_{q=-\infty}^{\infty}\sum_{r=-\infty}^{\infty}\varepsilon^p_{m-r,n-q}S^p_{yrq} + \frac{k_{xm}}{k_o^2}\left(k_{xm}S^p_{ymn} - k_{yn}S^p_{xmn}\right)$$

In (13), $\varepsilon^p_{m,n}$ and $\xi^p_{m,n}$ denote the Fourier components for the permittivity distribution, $\varepsilon^p(x,y)$, and the inverse permittivity distribution, $1/\varepsilon^p(x,y)$ of the p[th] layer given by

$$\varepsilon^p_{m,n} = \frac{1}{\Lambda_x\Lambda_y}\int_0^{\Lambda_x}\int_0^{\Lambda_y}\varepsilon^p(x,y)\exp(-j\left(\frac{2\pi mx}{\Lambda_x} + \frac{2\pi ny}{\Lambda_y}\right))dxdy \quad (14)$$

$$\xi^p_{m,n} = \frac{1}{\Lambda_x\Lambda_y}\int_0^{\Lambda_x}\int_0^{\Lambda_y}\frac{1}{\varepsilon^p(x,y)}\exp(-j\left(\frac{2\pi mx}{\Lambda_x} + \frac{2\pi ny}{\Lambda_y}\right))dxdy$$

For the geometries of interest here, shown in Figures 2 and 4, (14) can be solved analytically.

After substituting (14) into (13) and enforcing boundary conditions across all planar interfaces, an eigenvalue problem results that can be solved numerically for the reflected and transmitted diffracted orders $\vec{R}_{mn}$ and $\vec{T}_{mn}$. Our custom RCW code, developed using the Matlab™ programming environment, was used to calculate the complex transmission and reflection coefficients from woven fabrics.

B. Low Frequency Effective Electromagnetic Properties of Woven Structural Fabrics

At frequencies where the wavelength is much larger than the periodicity of the woven fabric ($\lambda_o >> \Lambda_x, \lambda_o >> \Lambda_y$) the electromagnetic properties of woven fabrics can be approximated by a bulk anisotropic permittivity derived using simple volume averaging. For the 1D unidirectional weaves, illustrated in Figure 2, the effective permittivity of the fabric is given as

$$\varepsilon_x^{(eff)} = \frac{W_x\varepsilon_x^{(x)} + (\Lambda_x - W_x)\varepsilon_{resin}}{\Lambda_x} \quad (15)$$

$$\varepsilon_y^{(eff)} = \frac{W_x\varepsilon_y^{(x)} + (\Lambda_x - W_x)\varepsilon_{resin}}{\Lambda_x}$$

where $\varepsilon_x^{(eff)}$ and $\varepsilon_y^{(eff)}$ denotes the effective permittivity of 1D weaves when the incident field is linearly polarized along the x and y axes respectively. Also in (15), $\varepsilon_x^{(x)}$ and $\varepsilon_y^{(x)}$ denotes the effective dielectric properties of the x-directed fiber bundles, described in (1), (2) and (3), and W_x and Λ_x denote the width of the fiber bundles and periodicity of the geometry of the fabric (illustrated in Figure 2), respectively.

For the 2D woven fabrics illustrated in Figures 3 and 4, the effective permittivity of the fabric is given by

$$\varepsilon_x^{eff} = \varepsilon_{resin} + \frac{\Lambda_x W_y \left(\varepsilon_x^{(x)} - \varepsilon_{resin}\right) + \Lambda_y W_x \left(\varepsilon_x^{(y)} - \varepsilon_{resin}\right)}{2\Lambda_x \Lambda_y}$$

$$\varepsilon_y^{eff} = \varepsilon_{resin} + \frac{\Lambda_x W_y \left(\varepsilon_y^{(x)} - \varepsilon_{resin}\right) + \Lambda_y W_x \left(\varepsilon_y^{(y)} - \varepsilon_{resin}\right)}{2\Lambda_x \Lambda_y} \tag{16}$$

where ε_x^{eff} and ε_y^{eff} denotes the low frequency effective permittivity of the 2D weaves when the incident field is linearly polarized along the x and y axes respectively.

4.0 Experimental Validation of Electromagnetic Model

To experimentally validate the performance of our model, we fabricated over 100 different samples and measured the transmissivity and reflectivity from 4-50 GHz.

A. Experimental Characterization

To measure the electromagnetic response of the samples over a broad frequency range, we employed the free-space focused beam approach illustrated in Figure 8, and described in numerous publications. To cover the entire 4-50 GHz frequency band, we varied the type and size of the antennas and lenses into four bands. Specifically, within the lower 4-18 GHz band we used a custom made focused beam system available at the Naval Surface Warfare Center, Carderock Division. This system integrates custom made large (~18" diameter) dielectric lenses to cover the lower frequencies range. Within the K-band (18-26 GHz), Ka-band (26-40 GHz) and U-band (40-50 GHz) we used commercial lens antennas purchased from QuinStar Technology, Inc. Using these systems we measured the transmittance of each sample using a Agilent PNA vector network analyzer and calibrated using Agilent's standard calibration kits. Time gating was used to remove undesirable reflections from the dielectric lenses and other components within the system. No other post-processing of the measurement data was conducted.

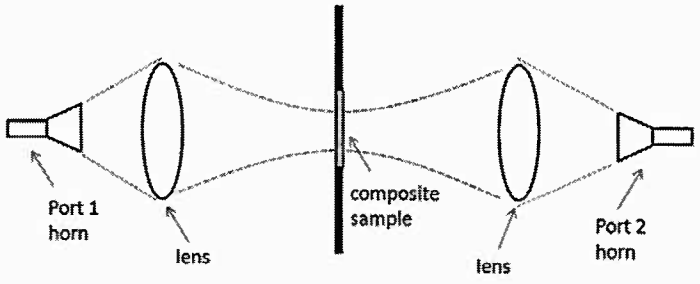

Figure 8. Free-space focused beam system used to characterize the electromagnetic properties of woven fabrics from 4-50 GHz.

B. SAMPLE PREPARATION

To validate the model presented here, over 100 different samples were prepared and tested. The samples varied in fiber and resin type as well as in bundle size and weave architecture. For all the samples characterized to date, the measured and modeled results show good agreement. For the sake of brevity, detailed results from five of the samples are presented here. Three of the five samples were a single ply of dry woven fabric (i.e. no resin) with different weave architectures. The other two were a single ply of the same woven fabrics infused with an epoxy vinyl ester resin (Derakane 510A) and cured. To create the infused samples, we used the standard vacuum assisted resin transfer molding (VARTM) process. All samples were mounted in 12"x12" frames and characterized using the free-space focused beam system.

Table 1 lists the relevant material and geometrical information from those samples. Table 3 presents the effective dielectric properties of the fiber bundles. The listed values are calculated using (2) and (3) and assuming a glass to resin volume fraction of 70% and the bulk dielectric properties given in Table 2. Here we assumed the bulk properties of the glass and resin to be frequency independent. However, since the RCW model is a frequency domain technique it can easily handle dispersive materials without modification.

Table 1. Composite samples used to validate EM modeling

	Sample1	Sample2	Sample3	Sample4	Sample5
fiber type	E-glass	E-glass	E-glass	E-glass	E-glass
resin type	no-resin (dry)	510A	no-resin (dry)	510A	no-resin (dry)
weave type	1D	2D plain weave	2D plain weave	2D plain weave	2D plain weave
Fabric weight (oz/yd^2)	16	18	18	24	24
W_x (mm)	1.6	4.4	4.4	4.6	4.6
Λ_x (mm)	1.9	4.5	4.5	5.3	5.3
W_y (mm)	NA	3.9	3.9	4.6	4.6
Λ_y (mm)	NA	6.6	6.6	6.6	6.6
thickness (mm)	0.4	0.7	0.7	0.7	0.7

Table 2. Bulk dielectric properties [www.agy.com]

	E-Glass	510A Resin
dielectric constant	6.2	3.0
tan(δ)	1.5e-3	1.67e-2

Table 3.Anisotropic effective media properties of the bundles

	Sample1	Sample2	Sample3	Sample4	Sample5
$\varepsilon_y^{(x)}$ and $\varepsilon_y^{(x)}$	3.04	4.93	3.04	4.93	3.04
tan(δ)	6.6e-4	6.9e-3	6.6e-4	6.9e-3	6.6e-4
$\varepsilon_x^{(x)}$ and $\varepsilon_y^{(y)}$	4.64	5.24	4.64	5.24	4.64
tan(δ)	1.5e-3	4.2e-3	1.5e-3	4.2e-3	1.5e-3
$\varepsilon_x^{(eff)}$	5.91	4.66	3.38	4.64	3.29
tan(δ)	6.8e-4	6.9e-3	1.2e-3	6.9e-3	1.2e-3
$\varepsilon_y^{(eff)}$	4.77	4.60	3.08	4.62	3.16
tan(δ)	8.4e-4	7.4e-3	9.7e-4	7.1e-3	1.3e-3

C. Results

In the following sections, experimental results for the samples described in Table 1 are compared to predicted results using both the low frequency effective media theory and our model based on the rigorous coupled wave algorithm. Results are provided for incident fields linearly polarized in the x and y directions with respect to the fabric geometry. This is illustrated in Figure 9.

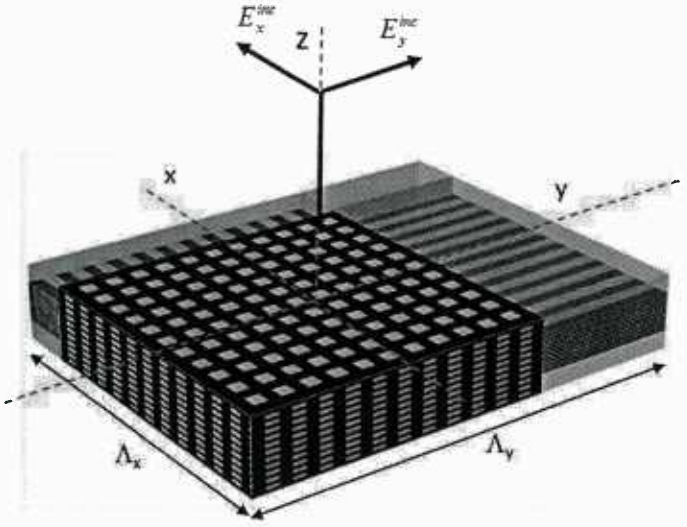

Figure 9. Coordinate system used to reference the polarization of the incident field with the principal axes of the samples measured.

Low Frequency Effective Media Model Results

Experimental results are first compared to the low frequency effective media approximations. The transmission coefficient, t, of the samples, assuming a bulk permittivity calculated using (15) or (16), is given as

$$t = \left(\frac{E_{transmitted}}{E_{incident}}\right) = \frac{2\sqrt{\varepsilon_{eff}}}{2\sqrt{\varepsilon_{eff}}\cos\left(\frac{4\pi f}{c}\sqrt{\varepsilon_{eff}}\,d\right) - j\left(1+\varepsilon_{eff}\right)\sin\left(\frac{4\pi f}{c}\sqrt{\varepsilon_{eff}}\,d\right)} \quad (17)$$

where c is the speed of light in a vacuum, f is the frequency, d is the thickness of the fabric layer and ε_{eff} is the effective permittivity calculated using either (15) or (16). The transmittance is the squared magnitude of the transmission coefficient given as

$$T = |t|^2 = \left|\frac{E_{transmitted}}{E_{incident}}\right|^2 \quad (18)$$

1) Unidirectional Fabrics

Figure 10 compares the experimental results to the low frequency effective media predictions, calculated from (17), for the single dry layer of unidirectional fabric that is described as sample #1 in Tables 1 and 2. It is not surprising that both the prediction and the experiment show a distinct anisotropic response. As presented in Table 2 , the dielectric constant of the fiber bundles has a significant polarization dependence

that will be reflected in the transmittance of the fabric. It is interesting, however, that the simple effective media equations do an adequate job of predicting the electromagnetic behavior of the unidirectional fabrics over the entire frequency band studied (4-50 GHz). As will be shown later, this is a direct result, of the small fiber bundle size (1.6 mm) and the tight spacing between fiber bundles (0.3 mm). While resonant effects are expected to occur they are likely to be seen beyond the frequency range studied.

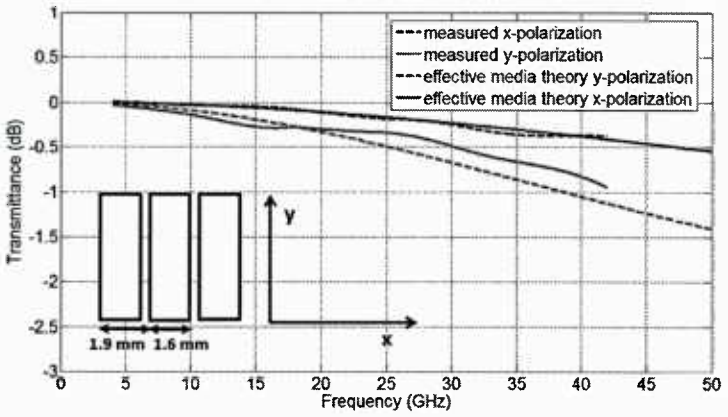

Figure 10. Effective media theory prediction and experimental results from sample #1 as a function of frequency and polarization. No resin for this sample.

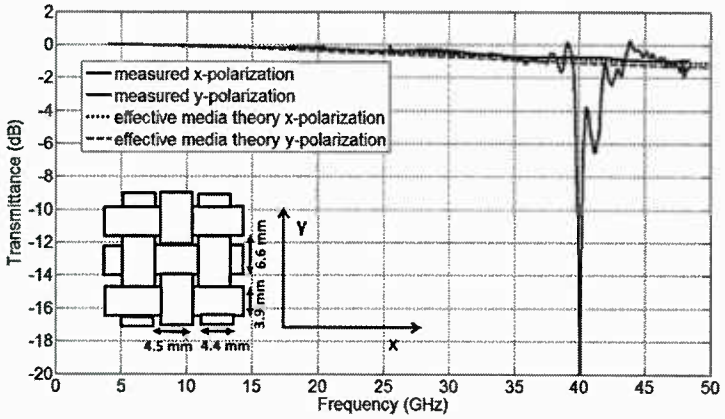

Figure 11. Effective media theory prediction and experimental results from sample #3 as a function of frequency and polarization. No resin for this sample.

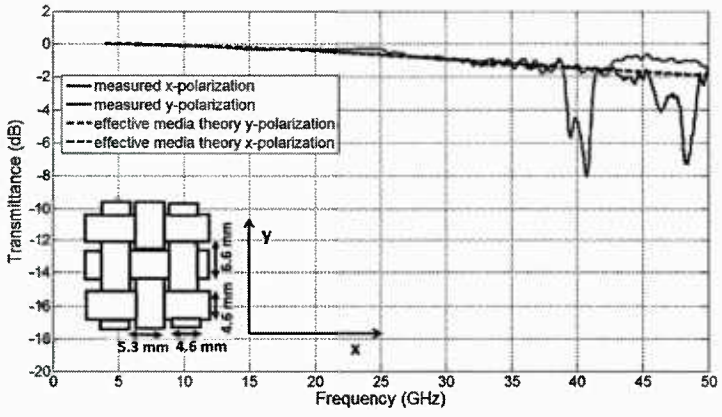

Figure 12. Effective media theory prediction and experimental results from sample #5 as a function of frequency and polarization. No resin for this sample.

2) TWO DIMENSIONAL WOVEN FABRICS

Figures 11 and 12 compare the experimental results to the low frequency effective media predictions for the single dry layer of fabrics described as samples #3 and #5 in Tables 1 and 3.

As with unidirectional fabrics, the effective media equations do a reasonable job of predicting the electromagnetic response up to approximately 30 GHz. Unlike the case with 1D fabrics, however, the anisotropic nature of the response is largely diminished. This is clearly an effect of having two sets of fiber bundles running in orthogonal directions.

An interesting effect that can be observed in the experimental results for the 2D fabrics is occurrence of large resonances beyond 30 GHz. These resonances, which are polarization sensitive, can significantly reduce the transmittance (-20dB) even for single layers of thin dry fabrics (i.e. fabrics that are much thinner than the wavelength). The polarization sensitivity of the response, shown very clearly in Figure 12, are due to the asymmetric properties of some of the fabrics. Later we will show that these resonances are in fact guided mode resonance (GMRs) effects. GMRs have been studied for some time within the optics community [19, 20] but, to the best of our knowledge; have never before been observed in woven glass fabrics or in structural composites. The exact spectral locations, amplitudes and polarization properties of these resonances are a function of the fabric's weave architecture, as well as the bulk dielectric properties of the fiber and resin used.

As a result of GMRs, simple effective media theory will not accurately predict the electromagnetic response beyond the frequency of the first guided mode resonance. For most structural fabrics, this occurs in the K to Ka band (18-35 GHz). However, for heavier fabrics in which the fiber bundles are larger and spaced further apart, the resonances can begin to occur at Ku or even within the X-band (8-18 GHz).

B. Rigorous Coupled Wave (RCW) Results

1) Normal Incidence Results

Figures 13 through 17 compare the predicted transmittance curves using the new hybrid electromagnetic model to the experimental results for samples #1-5. The transmittance was measured using the two orthogonal polarizations described in Figure 9 at normal incidence.

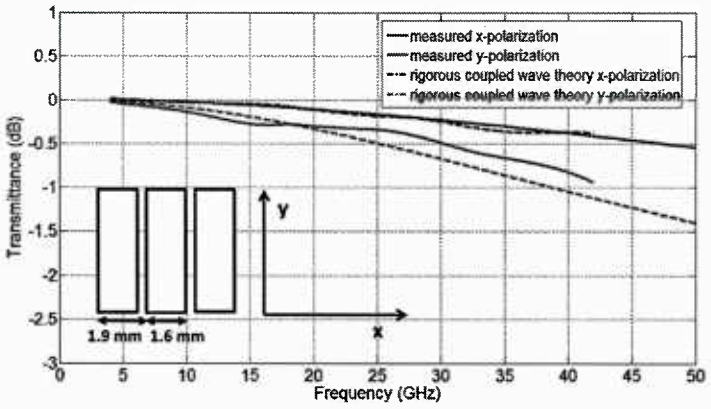

Figure 13. RCW predicted and experimental results from sample #1 as a function of frequency and polarization. No resin for this sample.

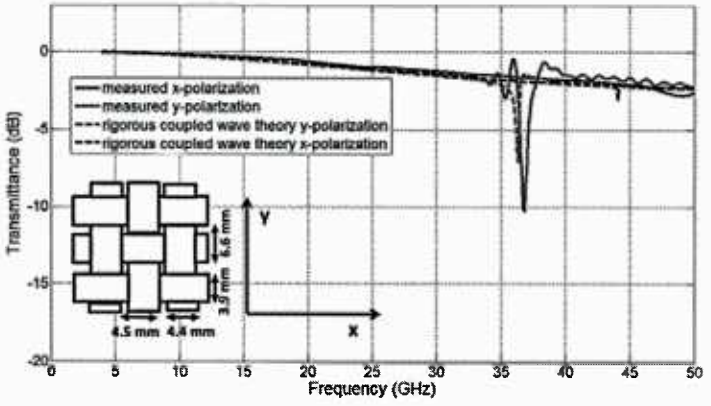

Figure 14. RCW predicted and experimental results from sample #2 as a function of frequency and polarization. Resin is 510A vinyl ester for this sample.

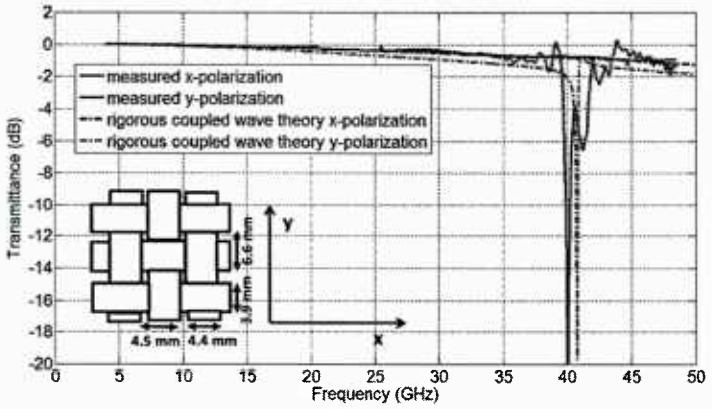

Figure 15. RCW predicted and experimental results from sample #3 as a function of frequency and polarization. No resin for this sample.

Figures 13 through 17 shows that our model adequately predicts the electromagnetic responses of all fabrics tested. This includes predicting the polarization dependent resonant effects seen at the higher frequencies. Comparing Figures 14 to 15 and Figures 16 to 17 also demonstrates how adding polymer resin to the fabric layers shifts the GMRs to lower frequencies and decreases their amplitudes without eliminating them completely. It should be noted the RCW calculations, shown in Figure 13 - 17, were computed in less than 30 seconds using a standard desktop computer. This is well over an order of magnitude faster than the same analysis using the finite element method (FEM). In the next section, we will provide a brief analysis of the resonant effects as well as some simple expressions to predict when they are likely to occur.

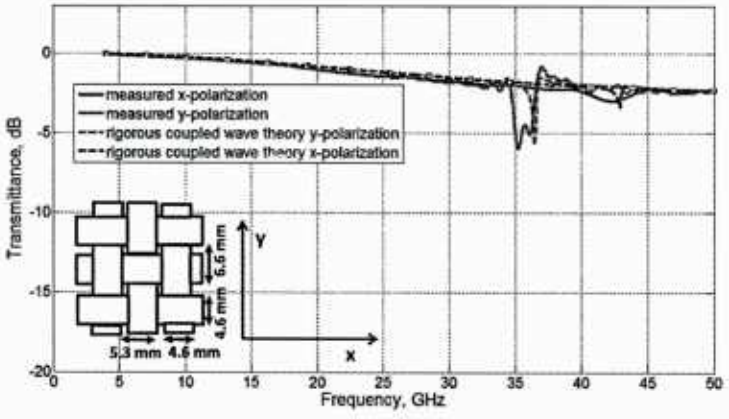

Figure 16. RCW predicted and experimental results from sample #4 as a function of frequency and polarization. Resin is 510A vinyl ester for this sample.

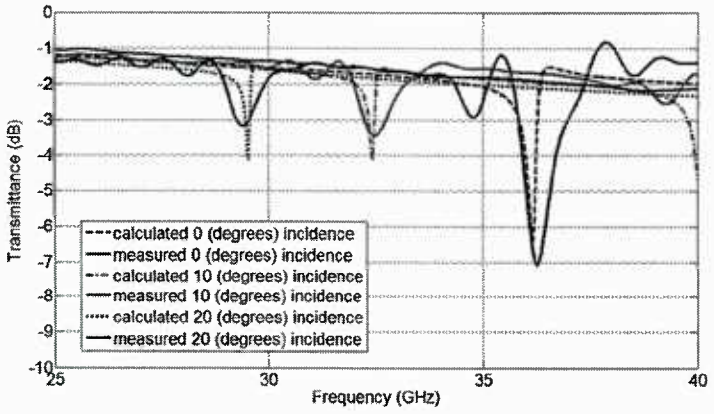

Figure 18. RCW predicted and experimental results from sample #2 as a function of frequency for several angles of incidence. Resin is 510A vinyl ester for this sample.

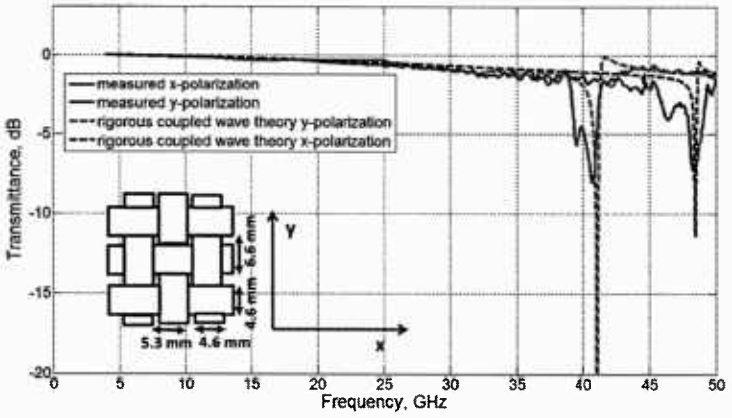

Figure 17. RCW predicted and experimental results from sample #5 as a function of frequency and polarization. No resin for this sample.

It should be noted that the measured results in Figures 16 and 17 reveal two closely spaced resonances for each of the two polarization states. This double resonance effect is not predicted by the model. We believe this effect is due to the fabric weaves not being perfectly periodic as assumed by the RCW model. A slight spatial variation in periodicity produces multiple closely spaced resonances in the measured results. Further investigation of this effect is needed to fully understand the discrepancy.

2) Variation with Incidence Angle

Figure 18 compares the calculated transmittance of sample #2 given in Table 1 as a function of incidence angle to the measured results. The elevation angle, $_{inc}$, was varied from 0° to 20°. As predicted by our model, and confirmed by measurements, the resonances shift towards lower frequencies as the incidence angle is increased. In the next section we will describe the physical nature of these observed resonances.

5. Electromagnetic Resonances within a Woven Fabric Composite

It has been shown that, within the microwave regime, common woven fabrics exhibit distinct electromagnetic resonances. These

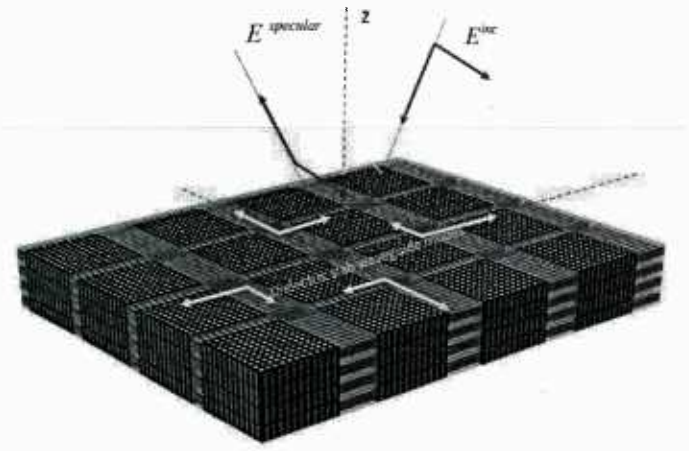

Figure 19. Illustration of guided mode resonances within a woven fabric composite. Transverse dielectric waveguide modes are excited within the fabric layer, or layers in the case of a laminate, and then reemitted, thus producing a strong specular reflection.

effects depend on the architecture of the weave as well as the bulk dielectric properties of the fiber bundles and resin. They have two likely causes: (1) Bragg resonances and (2) guided mode resonances. Bragg resonances occur in periodic structures when higher diffractive orders transition from evanescent to propagating modes. Since woven fabrics to a first order appear electromagnetically as 1D or 2D dielectric gratings, it is certainly possible that they could excite Bragg resonances.

It is straightforward to determine the minimum frequency at which the Bragg effects would occur since it is a simple function of the fabric's periodicity (i.e. Λ_x and Λ_y) and the incident angle illumination θ_{inc}. Specifically, the minimum Bragg frequency is given as

$$f_{min}^{Bragg} = \frac{300}{\max(\Lambda_x,\Lambda_x)(1+\sin(\theta_{inc}))} \text{ GHz} \quad (19)$$

For all fabrics studied in this project (see Table 1), we calculated the minimum Bragg frequency to always be greater than 45 GHz at normal incidence. However, our results demonstrate resonances well below 45 GHz. Moreover, our measured resonant frequencies vary significantly as the resin type is changed from air (i.e. no resin) to a polymer resin. Thus, the resonances we are observing are clearly not Bragg effects.

The second likely cause of the resonances is leaky guided mode resonances. A guided mode resonance (GMRs) is a phenomenon in which leaky dielectric waveguide modes are excited in the transverse plane of the fabric and then simultaneously reemitted (illustrated in Figure 19). At specific resonant frequencies, GMRs can produce very strong reflections in the specular direction.

To a first order, the guided mode resonant frequencies can be modeled by phase matching the Floquet modes of the dielectric grating (e.g. the fabric) with the transverse dielectric waveguide modes. The waveguide modes are calculated assuming a bulk effective permittivity of the fabric in the transverse plane. For the 2D woven fabrics, this results in the set of equations given in (20). These can be numerically solved for the resonant frequencies of the TE and TM dielectric waveguide modes. In (20) d is the thickness of the fabric layer, ε_{eff} denotes the effective permittivity calculated using (15) or (16), c is the speed of light in a vacuum, ϕ and θ are the incident angles shown in Figure 7 and f_o denotes the resonant frequency. For a given sample and incident field, the equations given in (20) can be solved numerically for all of the allowable GMR frequencies. The dominant (or lowest frequency) modes for our fabrics were the TE_{01} and TE_{10} modes for the x and y polarized incident field respectively. Table 4 compares the dominant guided mode resonant frequencies that were calculated using (20) with the measured resonant frequencies for samples #2 through #5.

(20)

$$\tan(\kappa_{pq} d) = \frac{2\kappa_{pq}\gamma_{pq}}{\kappa_{pq}^{\ 2} - \gamma_{pq}^{\ 2}} \qquad TM$$

$$\tan(\kappa_{pq} d) = \frac{2\varepsilon_{eff}\kappa_{pq}\gamma_{pq}}{\kappa_{pq}^{\ 2} - \varepsilon_{eff}^{\ 2}\gamma_{pq}^{\ 2}} \qquad TE$$

$$\kappa_{pq} = \sqrt{\varepsilon_{eff}\left(\frac{2\pi f_o}{c}\right)^2 - \beta_{pq}^{inc\,2}}$$

$$\gamma_{pq} = \sqrt{\beta_{pq}^{inc\,2} - \left(\frac{2\pi f_o}{c}\right)^2}$$

$$\beta_{pq}^{inc} = \sqrt{\left(\frac{2\pi f_o}{c}\sin(\theta)\cos(\phi) - p\frac{2\pi}{\Lambda_x}\right)^2 + \left(\frac{2\pi f_o}{c}\sin(\theta)\sin(\phi) - q\frac{2\pi}{\Lambda_y}\right)^2}$$

Table 4. Dominant resonant frequencies for both x and y polarization predicted using the RCW approach, GMR approach, Equation (20), and compared to measured results.

Resonant Frequencies (GHz) Sample Numbers from Tables 1 and 3						
	Sample #	1	2	3	4	5
Predicted (RCW) in GHz	x-polarization	127.3	*NA*	53.8	42.8	48.4
	y-polarization	132.3	36.2	41.0	36.5	41.0
Predicted GMR Theory in GHz	x-polarization	127.6	47.0	54.5	41.6	48.2
	y-polarization	133.4	36.1	40.1	35.2	40.1
Measured in GHz	x-polarization	*NA*	*NA*	*NA*	42.3	48.4
	y-polarization	*NA*	36.8	39.9	35.5	41.0

**note: NA in the above table occurs when either the resonant frequency is beyond our measurement range (4-50 GHz) or if a particular resonance was not detectable.*

As illustrated in Table 4 the approximate GMR approach was able to predict the dominant resonance frequencies of woven fabric composites within 10% of the RCW predictions and the measured results.

6.0 Conclusion

In this project we developed a new hybrid electromagnetic model that combined effective media theory with the rigorous coupled wave method to model the electromagnetic properties of woven fabric composites over a broad range of frequencies. We also fabricated a large number of test samples (>100)

to validate the model experimentally. The method was shown to accurately predict measured results including resonant effects not predicted using pure effective media theory. We also demonstrated, we believe for the first time, guided mode resonances that occur in standard structural grade woven composite fabrics and laminates. These resonances, which occur at subwavelength frequency, can be approximately modeled using simple dielectric waveguide theory.

7.0 Publications resulting from this project

1. M.S. Mirotznik, S. Yarlagadda, R. McCauley and P. Pa, 'Broadband Electromagnetic Modeling of Woven Fabric Composites', IEEE Microwave Theory and Techniques, Vol. 60, No. 1, January 2012, pp. 158-169.
2. M.S. Mirotznik, S. Yarlagadda, R. McCauley and P. Pa, 'Broadband Electromagnetic Modeling of Multilayered 3D Composite Laminates', Society for the Advancement of Material and Process Engineering, Baltimore MD, 2012
3. P. Pa, S. Yarlagadda, R. McCauley and M.S. Mirotznik, 'Electromagnetic Characterization of Embedded Frequency Selective Surfaces in a Structural Composite' Society for the Advancement of Material and Process Engineering, Baltimore MD, 2012